

# Preparation of Supercapacitors on Flexible Substrates with Electrodeposited PEDOT/Graphene Composites

Suvi Lehtimäki,<sup>\*,†</sup> Milla Suominen,<sup>‡</sup> Pia Damlin,<sup>‡</sup> Sampo Tuukkanen,<sup>†,§</sup> Carita Kvarnström,<sup>‡</sup> and Donald Lupo<sup>†</sup>

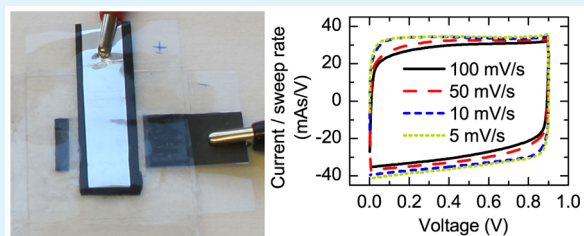
<sup>†</sup>Department of Electronics and Communications Engineering and <sup>‡</sup>Department of Automation Science and Engineering, Tampere University of Technology, 33720 Tampere, Finland

<sup>§</sup>Turku University Centre for Materials and Surfaces (MATSURF), Laboratory of Materials Chemistry and Chemical Analysis, University of Turku, 20014 Turun yliopisto, Finland

## Supporting Information

**ABSTRACT:** Composite films consisting of poly(3,4-ethylenedioxithiophene) (PEDOT) and graphene oxide (GO) were electrochemically polymerized by electrooxidation of EDOT in ionic liquid ( $\text{BMIMBF}_4$ ) onto flexible electrode substrates. Two polymerization approaches were compared, and the cyclic voltammetry (CV) method was found to be superior to potentiostatic polymerization for the growth of PEDOT/GO films. After deposition, incorporated GO was reduced to rGO by a rapid electrochemical method of repetitive cathodic potential cycling, without using any reducing reagents. The films were characterized in 3-electrode configuration in  $\text{BMIMBF}_4$ . Symmetric supercapacitors with aqueous electrolyte were assembled from the composite films and characterized through cyclic voltammetry and galvanostatic discharge tests. It was shown that PEDOT/rGO composites have better capacitive properties than pure PEDOT or the unreduced composite film. The cycling stability of the supercapacitors was also tested, and the results indicate that the specific capacitance still retains well over 90% of the initial value after 2000 consecutive charging/discharging cycles. The supercapacitors were demonstrated as energy storages in a room light energy harvester with a printed organic solar cell and printed electrochromic display. The results are promising for the development of energy-autonomous, low-power, and disposable electronics.

**KEYWORDS:** supercapacitor, flexible substrate, electrodeposition, graphene, PEDOT, composite, energy harvester



## 1. INTRODUCTION

The rise of ubiquitous, wearable, and flexible electronics brings challenges in the demand for new energy-storage solutions.<sup>1</sup> Supercapacitors, also known as electrochemical capacitors or ultracapacitors, are energy-storage devices that can be used in many such applications, especially when long cycle life, high power capability, and environmental friendliness are required. Compared to batteries, supercapacitors typically have lower energy densities but significantly longer cycle lives and can be rapidly charged and discharged.<sup>2</sup> An important advantage of supercapacitors in ubiquitous and disposable electronics is that they can be prepared from nontoxic materials.<sup>3</sup> Whereas commercial supercapacitors are produced as large, bulky devices with metal encasing, printable and flexible supercapacitors have also been demonstrated.<sup>4–7</sup> Such devices are ideal for use in, for example, energy harvesting<sup>8,9</sup> and Internet of Things applications.<sup>10</sup>

Depending on the charge-storage mechanism, supercapacitors can be classified into two types: electrical double-layer capacitors (EDLC) and pseudocapacitors.<sup>11</sup> EDLCs store and release energy based on the accumulation of charges at the interface between a porous electrode, typically a carbonaceous material with high surface area, and the electrolyte. In

pseudocapacitors, the mechanisms rely on fast and reversible Faradaic redox reactions at the surface and/or in the bulk, using materials such as transition metal oxides or electrically conducting polymers (ECPs).<sup>12</sup> Recently, more and more intensive efforts have been devoted to designing hybrid materials, such as composite materials of ECPs and different carbon materials, that can combine the advantages of both EDLC and the pseudocapacitor and meet the requirements of high energy density, high power density, and high cyclability.<sup>13,14</sup>

ECPs exhibit high redox capacitance and fast switching between redox states, making them interesting electrode materials for supercapacitor applications. Because of their inherent flexible polymeric nature, they have drawn a great deal of interest toward flexible supercapacitor applications. The redox process occurring during charging/discharging of an ECP is a combination of charge injection into the polymer backbone from the current collector and ion exchange from the electrolyte to maintain charge neutrality in the film. The rate

Received: February 19, 2015

Accepted: September 18, 2015

Published: September 18, 2015



of this charging/discharging is influenced by the mass transport of ions through the film, and therefore it is highly dependent on film morphology and type of electrolyte.

Polymer (PPy), polyaniline (PANI), and polythiophene (PT) as well as their derivatives are the most commonly used ECP materials for electrodes of supercapacitors. Their synthesis has been made using either chemical or electrochemical routes.<sup>15–18</sup> Chemical polymerization usually produces powdery materials and is the preferred technique for large-scale production of ECPs. Because the obtained materials show poor processing properties, they have to be functionalized in order to improve their solubility.<sup>19</sup> Thereafter films can be made using spin-coating or other solution-casting methods. In this process, the polymers are often mixed with binders and additives to construct the electrode. These will play an important role in device performance due to their high internal resistance. For direct growth of the ECPs on the current collector, the electropolymerization method is mostly used for supercapacitor applications, enabling an easy, one-step deposition method. In ECPs, a number of variables during electropolymerization, such as the polymerization method and nature of dopant and electrolyte to name a few, strongly affect the morphology of the film and in this way also influence the device performance.<sup>20,21</sup>

Ionic liquids (ILs) are becoming the solvent of choice in several chemical applications because they can replace common organic solvents that may be too volatile and/or hazardous.<sup>22</sup> From the electrochemical point of view, some ILs have excellent properties such as high ionic conductivity and a wide electrochemical potential window.<sup>23,24</sup> Some ionic liquids also show air and moisture stability, thus making them interesting electrolyte systems for the electropolymerization and charging/discharging of ECPs. Recent studies have shown that ECPs can be electropolymerized using ILs as dopant and electrolyte and that polymers have shown improved cycling stability in ILs and gel electrolytes compared to organic electrolytes.<sup>12,25–27</sup> This improved electrochemical performance and stability was mainly attributed to the lower volume changes observed for ECPs when using solvent-free electrolytes.

The common disadvantage of many ECPs, which has mitigated their use as sole supercapacitor materials, is their poor cycling stability. ECP electrodes exhibit large volume changes during the charging/discharging processes, leading to irreversible changes in 3-D structure, decreasing the electrochemical performance and stability. By preparation of polymer nanofibers, with porous capsular walls, such volume variations can be overcome, improving the cycling stability.<sup>28</sup> Studies using poly(3,4-ethylenedioxythiophene) (PEDOT) and structures similar to PEDOT, poly(3,4-alkylenedioxythiophenes) (PXDOTs), as charge-storage materials in electrochemical supercapacitors have reported on fast charge/discharge rates and lifetimes exceeding 50 000 cycles.<sup>29,30</sup> The formation of composites with, for example, carbon materials or metal nanoparticles can, in general, improve the stability of ECP supercapacitors by reducing the mechanical changes during charging and discharging.<sup>12,31–33</sup>

PEDOT and its derivatives have been widely studied and also lately used as charge-storage materials. Although PEDOT does not possess the highest specific capacitance of ECPs, it exhibits high conductivity, shows high chemical and thermal stability, and is electrochemically stable in a relatively wide potential window.<sup>34,35</sup> Electropolymerized PEDOT-based supercapacitors have been demonstrated to retain 80% of their capacitance

after 400 000 cycles when using ionic liquid and organic gel electrolytes.<sup>27</sup>

Graphene is considered a promising material candidate for electrochemical energy-storage devices because of its high accessible surface area, good mechanical strength, and high electrical conductivity, and it has also been used in composites with ECPs.<sup>36</sup> The mass production of supercapacitors based on ECP-graphene composites, however, requires low-cost nanomaterials. Graphene oxide (GO) has become the most common starting material for graphene-based applications because separated GO sheets can be produced in large quantities. For many applications, the reduction of GO, using chemical or electrochemical reduction or thermal annealing, is desired in order to restore the graphitic structure.<sup>37</sup> Of these reduction methods, the "green" electrochemical reduction is advantageous as it requires no oxidant or toxic reducing agents (e.g., hydrazine) and can be performed at room temperature.<sup>38</sup> In reduced graphene oxide (rGO), most of the oxygen functionalities are removed, but as a result, the sheets tend to restack as a graphite-like structure that shows low dispersibility in solvents. Aggregation of the rGO sheets reduces the available surface area and limits electron and ion transport, giving unsatisfactory capacitive performance.<sup>39</sup> Thus, one applied strategy has been the postreduction of ECP/GO composites in order to prepare uniform ECP/rGO materials, as it avoids the restacking of rGO sheets. In the literature, composite materials of ECPs together with graphene and GO have received a significant amount of attention in supercapacitor applications.<sup>40,41</sup> Composites have been prepared, for example, by sequential electropolymerization of PEDOT and electrical deposition of graphene,<sup>42</sup> spin-coating alternating PEDOT and graphene layers,<sup>43</sup> and chemical polymerization of PEDOT with functionalized graphene as counterion.<sup>44</sup>

In this work, conducting polymer composite films of PEDOT were electrochemically synthesized in the presence of GO in an easy one-step method directly onto graphite electrodes on flexible poly(ethylene terephthalate) (PET) substrates. Electropolymerization was performed in the ionic liquid 1-butyl-3-methylimidazolium tetrafluoroborate ( $\text{BMIMBF}_4^-$ ). PEDOT/reduced graphene oxide (PEDOT/rGO) composite films were prepared by inducing electrochemical reduction of GO incorporated into PEDOT as the dopant. The electrochemical reduction method is an environmentally benign approach that offers control of the reduction under mild reaction conditions. Moreover, ionic liquids show a broad potential window (5 V for  $\text{BMIMBF}_4^-$ ), thus allowing completeness of the reduction process not achievable with, e.g., aqueous electrolyte.<sup>45</sup> A study was performed comparing PEDOT/rGO composite films to those of pure polymer, focusing on redox behavior and morphological changes. The electroactivity of a PEDOT/rGO composite film increased considerably after the reduction process. A previous study focusing on the properties of the composite material when prepared on a small Pt electrode has been reported by the authors.<sup>46</sup>

Symmetric supercapacitors based on PEDOT, PEDOT/GO, and PEDOT/rGO composite films were assembled, and the devices were characterized following an industrial standard.<sup>47</sup> A nontoxic, neutral aqueous electrolyte was used in the supercapacitors. The supercapacitors assembled using PEDOT/rGO composite film showed the best capacitive performance, indicating the importance of the reduction process of GO on the overall electrochemical performance. The devices showed a capacitance value close to those reported

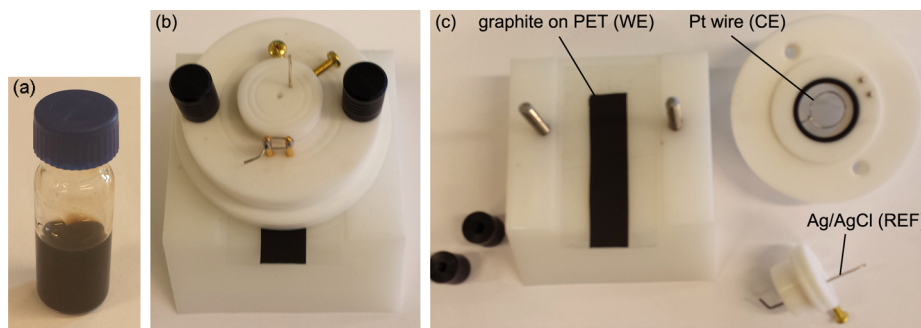


**Figure 1.** (a) GO/BMIMBF<sub>4</sub> dispersion ( $c_{\text{GO}} = 2.3 \text{ mg/mL}$ ) after 1 month from preparation. (b, c) Teflon cell used for the electropolymerization and characterization of films on a printed graphite electrode as working electrode (WE), Pt-wire as counter electrode (CE), and Ag/AgCl as reference electrode (REF). Images (b) and (c) show the cell when mounted and in parts, respectively.

for supercapacitors using PEDOT and ionic liquid electrolytes (10–20 mF/cm<sup>2</sup>).<sup>27</sup> Finally, it was also demonstrated that the fabricated supercapacitors can function as a power storage in an autonomous energy-harvesting circuit working in office lighting, where energy was harvested using a printed organic solar cell module.<sup>48,49</sup> Harvested energy was then used to power a printed electrochromic display,<sup>50</sup> the state of which could be updated over 50 times using a supercapacitor on a single charge. Considering the simplicity and short time for fabrication as well as the light weight and flexibility of the supercapacitors, the as-prepared composites show potential as power sources for use in low-power electronics.

## 2. EXPERIMENTAL SECTION

Current collector electrodes for the supercapacitors were prepared on poly(ethylene terephthalate) (PET, Melinex ST506, Dupont Teijin Films). First, 100 nm of silver was evaporated on the substrate. Two layers of graphite ink (Acheson Electrodag PF407C) were doctor blade coated on the silver, drying each layer for 5 min at 120 °C. The width of the graphite electrodes was 1.4 cm, while the silver layers were only 1.0 cm wide. The silver layers were needed due to insufficient conductivity of the graphite ink alone; the thick graphite layer protected the silver from the electrolyte in the supercapacitor.

GO was synthesized from graphite powder by the modified Hummers method<sup>51</sup> according to the procedure reported earlier.<sup>45</sup> The GO/IL dispersions were thereafter prepared using a solution mixing process (GO/H<sub>2</sub>O/IL) that after careful drying was used as electrolyte for the electropolymerization of composite films. The GO/IL dispersions were homogeneous and stable for several months, showing no aggregation (Figure 1a). UV-vis absorption spectroscopy was used to measure the GO concentration (2.3 mg/mL). A more detailed description on the preparation and characterization of the dispersions can be found elsewhere.<sup>46</sup>

In this work, electropolymerization and subsequent electrochemical studies were carried out using a three-electrode, one-compartment Teflon cell specially designed and compatible for PET substrates (Figures 1b and 1c). The graphite current collector on the flexible plastic PET substrate was used as a working electrode ( $A = 2.55 \text{ cm}^2$ ), Pt wire was used as a counter electrode, and a Ag/AgCl quasi-reference electrode was used as a reference electrode. The Ag/AgCl electrode was calibrated versus ferrocene (Fe/Fe<sup>+</sup>) ( $E_{1/2}(\text{Fe}/\text{Fe}^+) = 0.3 \text{ V}$ ) before each experiment. All potentials reported in this work are given versus this reference electrode. An Autolab PGSTAT101 or IviumStat potentiostat equipped with an impedance module was used for the electropolymerization and characterization studies.

Graphene oxide was synthesized from natural graphite flakes (Alfa Aesar, mesh 325, 99.8%). The ionic liquid, 1-butyl-3-methylimidazolium tetrafluoroborate (BMIMBF<sub>4</sub>, IoLiTec, 99%) was stored in an argon-filled glovebox. The monomer material 3,4-ethylenedioxythiophene (EDOT, Bayer) was stored in a refrigerator and

used as received. Ferrocene (Sigma-Aldrich, 98%) was used as received.

For the preparation of composite films, EDOT (0.1 M) was added to ultrasonicated (15 min) GO/IL dispersions. Also reference films without GO were prepared by adding EDOT (0.1 M) to plain IL. All solutions were deaerated by thorough purging with dry N<sub>2</sub> before the measurements. The polymer films were synthesized onto the graphite electrode on PET using both potential cycling and the potentiostatic method. In the cyclic voltammetry (CV) method, polymerization was carried out by continuous potential cycling between -1.0 and 1.2 V (15 cycles) using 50 mV/s scan rate. In the potentiostatic method, constant potentials of 1.00, 1.05, and 1.10 V were used for film formation. The number of cycles and the polymerization time were altered to ensure that, independent of the polymerization method, a constant charge for film formation (0.39 C/cm<sup>2</sup>) was always obtained. After each deposition, the polymer films were rinsed with plain IL to remove monomer and oligomer residues. The films on PET, used for the fabrication of the symmetric supercapacitors, were rinsed with ethanol and quartz-distilled water. For a set of the PEDOT/GO composite films, electrochemical reduction of incorporated GO to rGO was carried out in monomer-free BMIMBF<sub>4</sub> electrolyte by cycling the potential between -0.4 and -2.0 V using 50 mV/s scan rate (30 cycles). The deposited films (PEDOT, PEDOT/GO, and PEDOT/rGO) were then placed in monomer-free BMIMBF<sub>4</sub> to study the CV responses of the film-coated electrodes. The CVs were recorded between -0.4 to 0.8 V using 50 and 100 mV/s as scan rates. Cycling stability was also tested for 400 cycles.

Scanning electron microscopy (SEM) images of the films were obtained using a LEO 1530 Gemini FEG-SEM instrument. X-ray photoelectron spectroscopy (XPS) spectra were collected with a PerkinElmer PHI 5400 spectrometer. Raman experiments were performed by a Renishaw Ramascope (system 1000B,  $\lambda_{\text{exc}} = 514 \text{ nm}$ ) equipped with a Leica DMLM microscope and connected to a thermoelectrically cooled charged-coupled device (CCD) detector. The scattering signal was collected at 180° angle.

The supercapacitors were assembled by sandwiching two similar electrodes together with a separator paper (NKK TF4050) between them. The separator was soaked in aqueous 1 M NaCl. The electrodes were positioned in a 90° angle to each other, ensuring the overlap area was 2 cm<sup>2</sup>. The device was sealed with an adhesive film. A reference supercapacitor without the active layer, consisting only of the graphite electrodes, was assembled as well to observe the effect of the graphite on device capacitance.

The supercapacitors were characterized following an industrial standard,<sup>47</sup> which specifies a galvanostatic or constant current (CC) discharge test for capacitance and equivalent series resistance (ESR) determination.<sup>7</sup> Initially, the supercapacitors were cycled 20 times between 0 and 0.9 V to stabilize the polarization of the electrodes.<sup>52</sup>

The capacitance was measured by initially charging the capacitor to 0.9 V, holding the voltage for 30 min, and then discharging with a constant current. The capacitance was calculated from the voltage decrease rate between 80% and 40% of 0.9 V. The discharge current was from 50 to 70 μA/cm<sup>2</sup> depending on the device capacitance; the

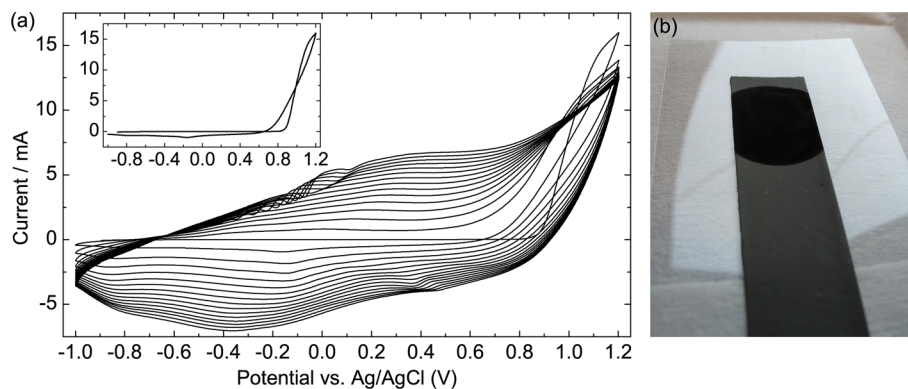


**Figure 2.** (a) Electropolymerization of PEDOT/GO onto a graphite–PET substrate by potential cycling between  $-1.0$  to  $1.2$  V (15 cycles,  $50$  mV/s) in a BMIMBF<sub>4</sub> solution containing GO ( $2.3$  mg/mL) and EDOT ( $0.1$  M). The inset shows the enlargement of cycle 1; axis labels are the same and omitted from the inset. During polymerization a total charge of  $1$  C was used ( $0.39$  C/cm<sup>2</sup>). (b) Photograph of the composite film on the graphite electrode on PET.

discharge current is specified in the standard as a function of the device capacitance.

The ESR was determined from a similar measurement as the capacitance, but at 10 times higher discharge current. The initial IR drop of the supercapacitor voltage divided by the current gives the ESR. The supercapacitors were also characterized with cyclic voltammetry in a two-electrode configuration from  $0$  to  $0.9$  V at voltage sweep rates  $5$ ,  $10$ ,  $50$ , and  $100$  mV/s. The devices were cycled four times at each rate prior to recording the final CV curve. The supercapacitors' cycling stability was tested by cycling the devices  $2000$  times at  $50$  mV/s between  $0$  and  $0.9$  V. The capacitance was measured again after cycling using the galvanostatic discharge test.

One fabricated PEDOT/rGO supercapacitor was demonstrated in a system with energy harvesting by a printed organic solar cell module (8 cells in series)<sup>48,49</sup> and display function by a commercial printed electrochromic display (ECD) from Acroo.<sup>50</sup> The supercapacitor was first charged with the solar cell in room light of  $\sim 750$  lx intensity (office computer work lighting, standard SFS-EN 12464-1) to over  $1$  V to ensure a fully charged device. The open circuit voltage of the solar cell in these conditions was  $2.45$  V. The solar cell was disconnected, and the supercapacitor was allowed to stabilize for  $1$  min. The supercapacitor was then used to switch the ECD on and off, manually connecting the supercapacitor electrodes to alternate electrodes of the ECD. The switching was done every  $2$  s, with the electrodes connected for  $1$  s and not connected for another second. The display was switched until the supercapacitor voltage had reached  $0.5$  V, at which point the display image was no longer sharp in the on state.

### 3. RESULTS AND DISCUSSION

#### 3.1. Optimization of Composite Film Properties.

Figure 2a shows the cyclic voltammograms recorded during electrochemical polymerization of a PEDOT/GO composite film using 15 cycles in the range of  $-1$  to  $1.2$  V and a scan rate of  $50$  mV/s. Growth of the film onto the graphite electrode can be nicely observed from the figure showing a clear increase in intensity of the oxidation and reduction peaks with the number of cycles. During the electropolymerization process, polymer deposition occurs during cathodic sweeping together with charged graphene nanosheets, intercalated with IL, functioning as charge-stabilizing counterions. The inset in Figure 2a shows the current response obtained during the first polymerization cycle. From this plot an oxidation potential of  $0.85$  V for EDOT can be observed. This value is in accordance to what has been reported for PEDOT and shows that no overpotentials are needed to perform electropolymerization of PEDOT in the GO/IL dispersions. The films showed good substrate adhesion, from one batch of dispersion and graphite electrode to another,

forming a homogeneous film covering the whole active working electrode area (Figure 2b). The influence of concentrations of GO in the electropolymerization of PEDOT/GO composite films has been studied in an earlier paper by the authors.<sup>46</sup> In these experiments the amount of GO in ILs was varied between  $0$  and  $4$  mg/mL, showing enhanced electrical film properties when the concentration of GO was fixed to  $2$  mg/mL.

Whereas potentiodynamic polymerization is carried out by scanning the potential within a certain potential region, galvanostatic and potentiostatic polymerizations are realized by controlling the anodic current and keeping the potential applied at a constant value, respectively. The method chosen will have considerable influence on film morphology and electronic properties as the polymerization mechanisms in all of the above-mentioned methods proceed in different ways. Therefore, electropolymerization using constant potential was also used for composite film synthesis and the film properties compared to those obtained using CV. The electropolymerization of PEDOT/GO was carried out at  $1.00$ ,  $1.05$ , and  $1.10$  V. When using increasing potentials for film formation, the adhesion onto the electrode substrate was considerably depressed, even leaving substantial parts of the electrode surface uncovered (Figure S1 in the Supporting Information). If using lower potentials ( $0.95$  V), no film formation was observed even when prolonging the polymerization time. Figure 3 shows a comparison in electroactivity of the composite films when prepared using these two polymerization methods. According to the CVs in Figure 3, the oxidation and reduction currents for the composite film are substantially lowered when it had been polymerized using the potentiostatic method. This

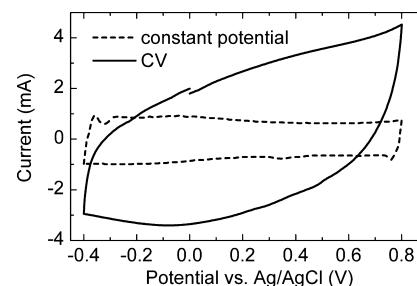


**Figure 3.** CVs in BMIMBF<sub>4</sub> at  $50$  mV/s of PEDOT/GO composite films electropolymerized using the CV method (solid line) and the constant potential method at  $1.0$  V (dashed line).

is mainly due to the properties of the electrode substrate: a fair amount of material is produced also in the potentiostatic method, but most of it remains in the polymerization solution and does not adhere to the electrode surface. Therefore, in all further studies of composite film properties and for making the batches of composite films to be used in supercapacitor devices, the CV method was chosen as the polymerization method. When water was used as electrolyte in the polymerization process, film adhesion onto the electrode substrate was poor and independent of the polymerization method used.

**3.2. Electrochemical Reduction of PEDOT/GO Composite Films.** In recent literature related to graphene-based supercapacitors, GO has usually been reduced with the aid of chemical or thermal methods.<sup>53,54</sup> In composite structures such a reduction process could result in polymer degradation arising from the reducing agents and high processing temperature. Even when using milder reductants such as NaBH<sub>4</sub>, a decrease in the electrochemical activity of PEDOT/GO composite films could be found after a short 10 min reduction time.<sup>55</sup> The electrochemical reduction method has been introduced as a fast and environmentally friendly way for producing a partly recovered sp<sup>2</sup> lattice.<sup>45,56</sup> Especially the combination of spectroscopy with the electrochemical method gives a unique possibility to simultaneously control and follow the evolution of oxygen-containing defects with the reduction potential.<sup>57</sup> Such spectroelectrochemical results have indicated that changes in GO structure take place in a quite narrow potential range extending from -1 to -1.7 V (vs Ag/AgCl).<sup>58</sup> In this work, PEDOT and PEDOT/GO films were electrochemically reduced by the CV method in the potential range -0.4 to -2.0 V using 50 mV/s and 30 reduction cycles. CV and impedance spectroscopy characterizations for PEDOT/GO composite films have shown that, when the number of electroreduction cycles was altered from 10 to 30 cycles, the highest electrochemical activity was obtained upon extending the number of reduction cycles to >20.<sup>46</sup>

The CVs in Figure 4 show the charging/discharging process in BMIMBF<sub>4</sub> for PEDOT and PEDOT/GO directly after

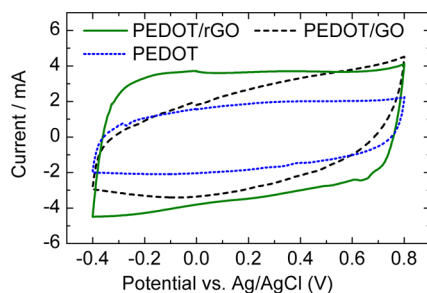


**Figure 4.** CVs in BMIMBF<sub>4</sub> for PEDOT (blue dotted line), PEDOT/GO (black dashed line), and PEDOT/rGO (green solid line) films. The scan rate was 50 mV/s.

polymerization and for the PEDOT/GO film after electrochemical reduction to PEDOT/rGO. PEDOT is one of the few examples of ECPs that is both p- and n-dopable, which is why electroreduction shows no degradation on electroactivity.<sup>25</sup> After electrochemical reduction, the oxidation and reduction currents for the composite films were substantially enhanced, showing a more rectangular-shaped capacitive CV response (Figure 4). The CVs are not perfectly rectangular, but this is seldom the case for pseudocapacitive materials such as ECPs.

The electroactivity of PEDOT itself is stable when comparing films before and after reduction ( $Q = 550$  and  $560 \mu\text{C}$ , respectively), which is why this enhancement must be due to GO incorporated during film synthesis. The long-term charging/discharging process is a detrimental issue in supercapacitor applications. For plain PEDOT films, 12% fall in charge retention was obtained after 400 cycles whereas the composites showed, under the same experimental conditions, just 6% decrease. The CVs from the stability measurements are shown in Figure S2 (Supporting Information). The results indicate an enhancement in the mechanical and chemical stability of the composite materials compared to the pristine PEDOT polymer.

Spectroscopy techniques, such as Raman and IR, are frequently used for the characterization of carbon-based materials and graphene structures in particular and to verify incorporation of GO and graphene into ECP films.<sup>59–62</sup> The Raman spectra of a drop-cast film of GO and that of PEDOT/GO electrochemically polymerized in BMIMBF<sub>4</sub>, using the excitation at  $\lambda_{\text{ex}} = 514 \text{ nm}$ , are shown in Figure S3 (Supporting Information). For GO the important features observed in the Raman spectra are the D and G bands at  $1354$  and  $1599 \text{ cm}^{-1}$ , respectively.<sup>51</sup> For PEDOT/GO, two strong bands at  $1509$  and  $1430 \text{ cm}^{-1}$  are attributed to C=C and C=C–O stretching in PEDOT, respectively. There is a small red-shift observed in these bands when compared to that observed for the PEDOT film without GO, indicating  $\pi$ - $\pi$  interactions of PEDOT chains with GO sheets. This together with the hump in the composite spectrum at  $1600 \text{ cm}^{-1}$  further verifies the presence of GO in the composite films. Because of the strong overlap between PEDOT and GO bands, it was not possible from the Raman spectra to make any analysis of the D/G ratios upon electrochemical reduction of the composite films that would tell about the recovery of order in graphene.<sup>38</sup>

The recovery order can be examined, however, using the XPS spectroscopy technique by looking at the decrease in the amount of oxygen groups upon electroreduction. Furthermore, this technique confirmed successful formation of composite structures. The atomic composition (%) from the XPS fitting showed the following change in the C/O ratio for PEDOT (9.97), PEDOT/GO (5.67), and PEDOT/rGO (11.49). The decrease in the C/O ratio for the composite materials indicates GO incorporation, and after reduction the increase in the C/O ratio is due to the removal of oxygen-containing surface groups from GO. Our previous study on PEDOT/GO composite structures using IR spectroscopy as a characterization method showed that the bands from PEDOT and GO were overlapping to such an extent that the presence of GO and furthermore deoxygenation of the GO platelets after electrochemical reduction could not be confirmed by using this technique.<sup>46</sup> In any case, the IR results indicated successful formation of the composite in the IL/GO dispersion.

Masses for these electrochemically polymerized films on printed graphite electrodes were so small that it was impossible in this work to obtain any reliable specific capacitance (F/g) values. However, film production was reproducible due to the confined electrode area (Figure 1,  $2.55 \text{ cm}^2$ ). The areal capacitance was therefore reported in this work and obtained by dividing the charge passed during film charging (second scan) by the voltage window and area of the film, which was  $2.55 \text{ cm}^2$  in the 3-electrode setup and  $1.96 \text{ cm}^2$  in the 2-electrode setup. The 2-electrode value corresponds to the electrode overlap area in the assembled supercapacitor

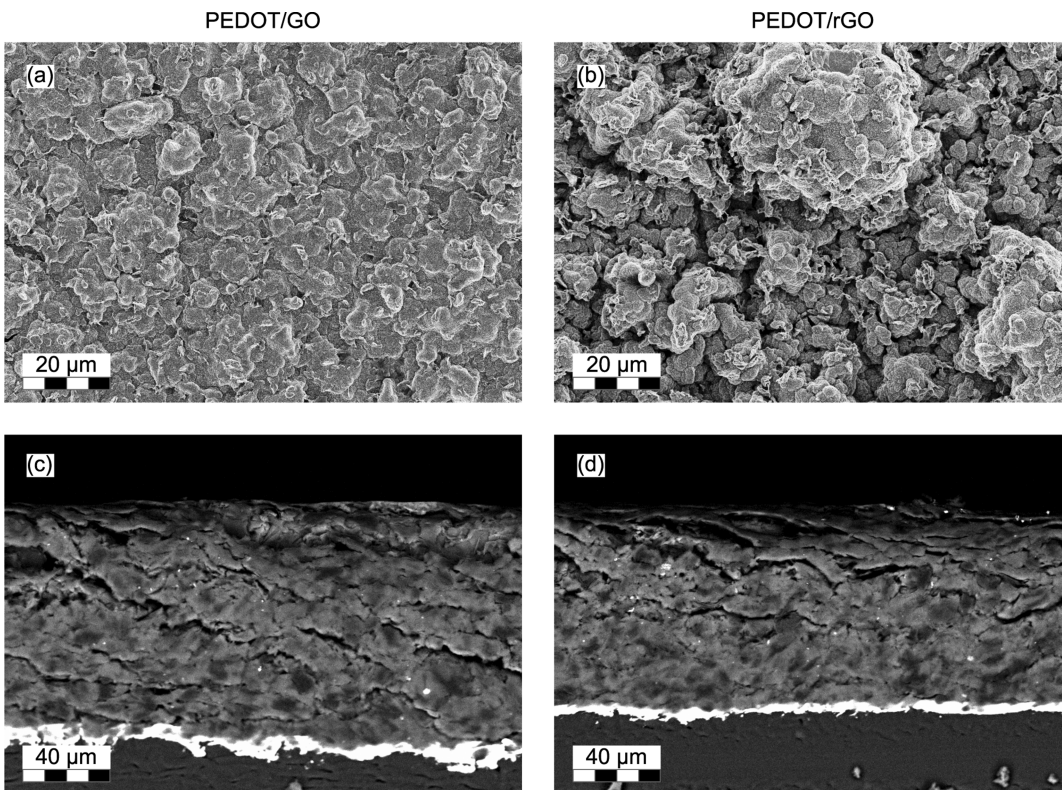


**Figure 5.** SEM images of PEDOT/GO (a) and PEDOT/rGO (b) composite films with 1 000 $\times$  magnification. Images (c) and (d) show the cross section with 500 $\times$  magnification.

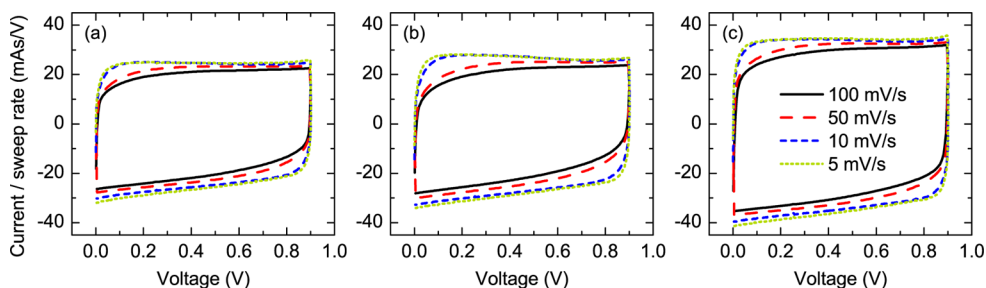


**Figure 6.** CV curves of supercapacitors, normalized to voltage sweep rate: (a) PEDOT, (b) PEDOT/GO, (c) PEDOT/rGO. The axis and curve labels are the same for all graphs.

structure. The calculated areal capacitances in the ionic liquid electrolyte for PEDOT, PEDOT/GO, and PEDOT/rGO in the 3-electrode setup were on average 11, 16, and 25 mF/cm<sup>2</sup>, respectively. These results show that reduction of the composite film increases the capacitance value.

**3.3. SEM Analysis.** The SEM images in Figure 5 show the morphology for the PEDOT composite films directly after electropolymerization (PEDOT/GO) and after 30 reduction cycles in BMIMBF<sub>4</sub> (PEDOT/rGO). As for electrochemically polymerized conducting polymers, the composite films show a 3D morphology with an interconnected network of grains and pores. Additionally, there are crumpled flakes embedded in the polymer matrix, which can be clearly observed from the magnification in Figure S4 (Supporting Information). These images also show that the ECP effectively prevents the stacking of rGO. It can also be seen that the composite displays an open structure permitting electrolyte movement.

From the cross-sectional images in Figure 5c and d, taken in backscattering mode, an average layer thickness of 110  $\mu\text{m}$

could be observed for PEDOT/GO and 90  $\mu\text{m}$  for PEDOT/rGO; this value includes also the graphite ink on the PET substrate with a thickness of  $\sim$ 25  $\mu\text{m}$ . The cross-sectional view reveals an indistinguishable microstructure showing no indication of sheetlike stacking of graphene flakes.

Electropolymerization of PEDOT/GO composite materials onto the graphite electrodes on flexible PET substrates using water/GO as electrolyte was also performed. Interestingly, the physical appearance of the composite changed drastically when using GO/H<sub>2</sub>O dispersions for electropolymerization of the composite material. In this case, the obtained film had a crumpled sheetlike appearance showing no network formation between the polymer and the GO sheets (Figure S5 in the Supporting Information).

A relatively thick film is needed for sufficient capacitance in the assembled supercapacitors. Moreover, films that are too thin may give an overstatement of the material's performance in the application; commercial supercapacitors are constructed with active material thicknesses ranging from ten to several

hundred micrometers.<sup>52</sup> However, the light weight and flexibility aimed for in the plastic supercapacitors also limit the maximum thickness of the film.

**3.4. Characterization of the Supercapacitors.** The supercapacitors were characterized according to an international standard,<sup>47</sup> as the goal of the work was to demonstrate the applicability of the composite devices. The devices were also characterized with the CV method to obtain a qualitative view of device properties and to facilitate comparison with the 3-electrode measurements and previous literature reports. Using a 2-electrode cell configuration should lead to more realistic results, predicting the performance of the materials in an actual application.<sup>52</sup>

The CV curves at different sweep rates for PEDOT, PEDOT/GO, and PEDOT/rGO are shown in Figure 6. The curves are normalized to voltage sweep rate, which enables comparison of different rate curves as well as gives an approximation of the capacitance. The CV curves for all materials are rectangular, which indicates that the material charges and discharges quickly and efficiently. More curvature at the corners at higher sweep rates is caused by the ESR of the device.<sup>27</sup> The shapes can be better compared through the fill factor, which is the area of the CV curve divided by the area of the smallest rectangle enclosing the curve.<sup>27</sup> The fill factors of the 100 mV/s curves are 81% for PEDOT, 79% for PEDOT/GO, and 84% for PEDOT/rGO. While the differences are not substantial, PEDOT/GO does yield the lowest fill factor, indicating a higher ESR; this is expected due to the poor conductivity of unreduced GO, where the planar sp<sup>2</sup> structure of graphene is broken.

The capacitances obtained from the CV curves are listed in Table 1 (calculated from the charging phase of the curve). The

**Table 1. Single Electrode (se) and Supercapacitor (dev) Capacitances in mF/cm<sup>2</sup>, Obtained from CV Curves with 100 mV/s Sweep Rate**

	PEDOT	PEDOT/GO	PEDOT/rGO
C <sub>se</sub> in IL	11	16	25
C <sub>dev</sub> in NaCl (aq)	10	10	14

capacitances of the devices were 10 mF/cm<sup>2</sup> for both PEDOT and PEDOT/GO and 14 F/cm<sup>2</sup> for PEDOT/rGO. Figure 7 shows the change in calculated capacitance at different voltage sweep rates. The capacitance obtained from the 100 mV/s CV curve for PEDOT is similar to that reported in ref 27, where 10 mF/cm<sup>2</sup> was also obtained for a symmetric supercapacitor with 100 mV/s sweep rate with a polymerization charge

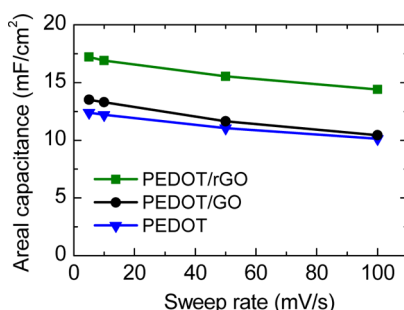


**Figure 7.** Capacitance calculated from the CV curves against the voltage sweep rate for 2-electrode symmetric supercapacitors.

approximately similar to that used here, although the electrolyte was different.

Table 2 lists the results from the supercapacitor characterization. The constant current results are obtained from the

**Table 2. Supercapacitor Properties of Samples with Symmetric 2-Electrode Configuration and NaCl(aq) Electrolyte, Obtained from Galvanostatic Discharge**

	PEDOT	PEDOT/GO	PEDOT/rGO
C (mF/cm <sup>2</sup> )	14	14	18
Change in C after 2000 cycles	-6.9%	-5.4%	-6.8%
ESR (Ω)	26	43	25

measurements according to the standard,<sup>47</sup> which specifies a discharge current that depends on the capacitance of the device. The discharge currents were thus slightly different for the different samples, but in the range of 50–70 μA/cm<sup>2</sup>. As expected, the ESR was highest with PEDOT/GO because of the poor conductivity of GO. As PEDOT and PEDOT/rGO had similar ESRs, the rGO does not seem to affect the conductivity in the active electrode notably. On the other hand, the supercapacitor structure with printed graphite layers and the separator may be the most significant sources of ESR in any case. Discharge curves are shown in Figure S6 (Supporting Information).

It appears that the incorporation of GO does not contribute to the capacitance of the film in the symmetric supercapacitors, which indicates that PEDOT is the main source of capacitance in both PEDOT and PEDOT/GO samples. While GO may increase the surface area of the composite compared to bare PEDOT, the poor conductivity could make parts of the electrode inaccessible to electronic charges. Reducing the GO, however, increases the capacitance, because the rGO conducts better and can thus participate in double-layer formation.

The difference in capacitances of PEDOT and PEDOT/GO between 2- and 3-electrode measurements is interesting. Although the capacitances themselves cannot be directly compared due to the different electrolytes and voltage ranges, the trends between samples can. The electrolyte may change the electrochemistry of ECPs, but ion sizes can affect the results as well. The latter may explain the different effect of the incorporation of GO into PEDOT measured in ionic liquid, where it improves the capacitance compared to PEDOT, and in aqueous NaCl, where it does not have an effect. Solvated Na<sup>+</sup> and Cl<sup>-</sup> ions are smaller than the bulky ions of the ionic liquid: this may allow them to fit in the porous structure of the PEDOT layer better compared to the ionic liquid. If the poorly conducting GO does not contribute to double-layer formation, the capacitance should then be similar regardless of its presence when NaCl(aq) is used. The GO may nevertheless affect the morphology of the film, allowing also the larger ionic liquid ions better access to the active ECP, which can account for the improved capacitance of the PEDOT/GO compared to bare PEDOT.

The voltage range of individual electrodes is another factor that affects the capacitance.<sup>63</sup> In the 3-electrode CV curves for PEDOT, however, the capacitance appears fairly constant with potential (Figure 4), so the effect may not be as pronounced as in ref 63.

As the mass of the films was too small to weigh reliably, specific capacitances in F/g cannot be calculated. However, the energy and power densities can be estimated through the

thickness obtained from the SEM images. The thickness of PEDOT/GO was  $\sim 85 \mu\text{m}$  and that of PEDOT/rGO was  $65 \mu\text{m}$ . The energy density is thus  $0.7 \text{ J/cm}^3$  for PEDOT/GO and  $1.2 \text{ J/cm}^3$  for PEDOT/rGO. The larger energy density of PEDOT/rGO is due to not only the larger capacitance but also the composite shrinking somewhat during the reduction. The power densities are  $0.29$  and  $0.63 \text{ W/cm}^2$  for unreduced and reduced composite, respectively. The larger ESR of PEDOT/GO contributes to the lower power density in this case.

Cycling the supercapacitors 2000 times lowered the capacitance by 5–7% in all the samples. Figure 8 shows the

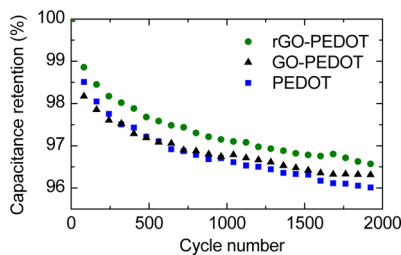


**Figure 8.** Capacitance of the supercapacitor devices during cycling, calculated from the CV curves.

capacitance retention as calculated from the CV curves; the capacitance drop listed in Table 2 is calculated from a constant current discharge test before and after the cycling. The capacitance falls quickest initially with PEDOT/GO but stabilizes better than with PEDOT or PEDOT/rGO. The measurement method also affects the results: based on the constant current method, the capacitance retention is best in PEDOT/GO, although CV shows PEDOT/rGO to be the best. One reason for this may be electrochemical reduction of GO on one of the electrodes both during cycling and the 30 min potential hold before discharge; however, the differences between the materials are too small in this case to draw a definitive conclusion.

The change in capacitance during cycling is more than that observed in PEDOT supercapacitors with ionic liquid electrolyte<sup>27</sup> but of similar magnitude with other aqueous electrolyte devices.<sup>13,64</sup> The difference is due to the better cycling stability of ECP electrodes in ionic liquid electrolytes.<sup>12</sup> The difference in electrolyte may also be the reason for the similar capacitance retention of the aqueous devices with different materials, whereas the composite formation improved the retention in 3-electrode measurements in IL.

Similar supercapacitor devices have been previously prepared by the authors using carbon nanotubes as the electrode material but the same electrolyte, substrate, and device size.<sup>7</sup> There, a capacitance of  $6 \text{ mF/cm}^2$  was achieved, which is far lower than what was obtained with the composite materials in this work.

To determine if the graphite current collector contributed to the capacitance, a device was assembled with only the current collector electrodes. The obtained CV curve of the device at  $100 \text{ mV/s}$  is shown in Figure S7 (Supporting Information). Clearly, the capacitance of the graphite is minute, with the calculated capacitance from the CV curve being  $5 \mu\text{F}$ . Thus, all of the capacitance of the devices with electropolymerized layers results from the ECP or the composite.

**3.5. Demonstration with Solar Cell and Electrochromic Display.** A PEDOT/rGO supercapacitor was used in a simple demonstration of an energy-harvesting system (Figure 9a and b). An organic printed solar cell module<sup>48,49</sup> was

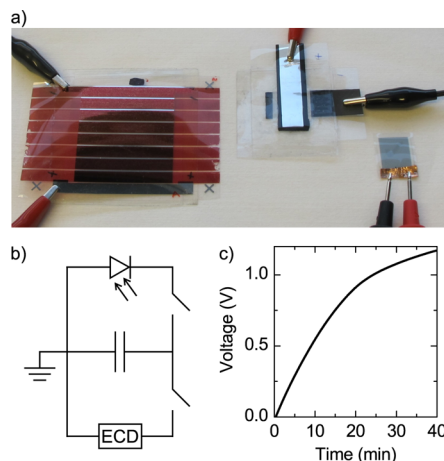


**Figure 9.** (a) Setup of the supercapacitor demonstration with a solar cell and electrochromic display. (b) Circuit diagram of the setup. (c) Voltage over the supercapacitor when charging with the solar cell.

used first to charge the supercapacitor in ambient room lighting; the charging curve is shown in Figure 9c. As only indoor lighting was used, the supercapacitor was charged slowly. The charging was quickest in the beginning. This can be expected, as the current from the solar cell is close to its short-circuit current when the voltage over it is low. As the voltage of the supercapacitor rises, the solar cell current is reduced and the charging becomes slower.

The supercapacitor was then disconnected from the solar cell module and connected to the ECD. The connection was reversed every 2 s to switch the display on and off. Figure 10a

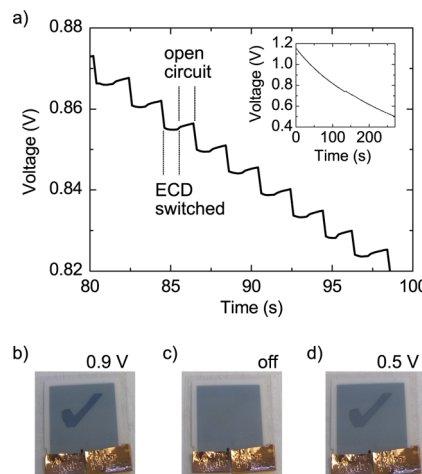


**Figure 10.** (a) Voltage over the supercapacitor during the switching demonstration. The entire measurement range is displayed in the inset. (b) ECD turned on with  $0.9 \text{ V}$  from the supercapacitor. (c) ECD turned off with  $-0.5 \text{ V}$ . (d) ECD turned on with  $0.5 \text{ V}$ .

presents the voltage over the supercapacitor during the switching. The voltage falls  $\sim 6 \text{ mV}$  each time the display is switched; the fall is of similar magnitude regardless of switching direction. The ECD was switched on and off  $\sim 65$  times until the voltage across the supercapacitor dropped to  $0.5 \text{ V}$ , at which point the ECD no longer switches completely (Figure 10b–d).

The switching is rapid: no significant difference was observed visually between switching with the supercapacitor versus

switching with a potentiostat. The voltage does not fall further during the 1 s the supercapacitor is kept connected to the ECD. This indicates that the supercapacitor is able to supply enough current instantaneously for the display to be switched. During the 1 s open circuit, the supercapacitor voltage rises slightly. This can be explained with charge redistribution in the supercapacitor electrodes, modeled as parallel resistive capacitive (RC) branches with different time constants:<sup>65,66</sup> the electrodes discharge unevenly, with the slower parts compensating charge to the quicker ones after the initial discharge.

The demonstration shows the applicability of these supercapacitors in an energy-harvesting system. Ambient indoor light is enough to charge the device with an organic solar cell in well under 1 h. Combined with suitable low-power silicon-based control circuits, energy-autonomous, distributed, and disposable devices can be realized.

#### 4. CONCLUSIONS

We have demonstrated that GO can be incorporated into PEDOT films by a simple electropolymerization method on flexible substrates and can be further reduced by electrochemical reduction to rGO. Potentiostatic and CV polymerization methods were compared, and the cyclic approach was found to be better with the printed substrates due to better adhesion of the composite film. The films showed good capacitive properties that can be ascribed to the large accessible surface area of rGO combined with the pseudocapacitance of PEDOT.

The films were prepared in an ionic liquid to facilitate good film formation and thorough reduction of the GO. Supercapacitors were then assembled with aqueous NaCl electrolyte, which is a safe and simple option for disposable supercapacitors. The symmetric devices had good capacitive properties as well as cycling stability. The supercapacitors were also demonstrated as part of an energy-harvesting system running a small electrochromic display. Using supercapacitors as an intermediate storage of energy allows a system to keep functioning with the primary energy source not available. Moreover, all the components used here can be mass-produced on flexible substrates, facilitating a low-cost solution to many applications in distributed electronics.

#### ■ ASSOCIATED CONTENT

##### Supporting Information

The Supporting Information is available free of charge on the ACS Publications website at DOI: [10.1021/acsami.5b05937](https://doi.org/10.1021/acsami.5b05937).

Photographs of potentiostatically polymerized films, CV curves of cycling stability test, Raman spectra, additional SEM images, galvanostatic discharge curves, CV curve of graphite reference device ([PDF](#))

#### ■ AUTHOR INFORMATION

##### Corresponding Author

\*Phone: +358 40 849 0623 E-mail: [suvi.lehtimaki@tut.fi](mailto:suvi.lehtimaki@tut.fi)

##### Notes

The authors declare no competing financial interest.

#### ■ ACKNOWLEDGMENTS

The authors acknowledge the Academy of Finland for its financial support under Grant nos. 139881 and 264743. The authors thank Päivi Apilo and Sanna Rousu at VTT for

providing the printed solar cell module, Acreo for providing the ECD, and Markku Heinonen for assistance with the XPS measurements. S.L. thanks the Foundation of Nokia Corporation for support.

#### ■ REFERENCES

- Zhan, Y.; Mei, Y.; Zheng, L. Materials Capability and Device Performance in Flexible Electronics for the Internet of Things. *J. Mater. Chem. C* **2014**, *2*, 1220–1232.
- Kötz, R.; Carlen, M. Principles and Applications of Electrochemical Capacitors. *Electrochim. Acta* **2000**, *45*, 2483–2498.
- Jost, K.; Stenger, D.; Perez, C. R.; McDonough, J. K.; Lian, K.; Gogotsi, Y.; Dion, G. Knitted and Screen Printed Carbon-Fiber Supercapacitors for Applications in Wearable Electronics. *Energy Environ. Sci.* **2013**, *6*, 2698–2705.
- Shi, S.; Xu, C.; Yang, C.; Li, J.; Du, H.; Li, B.; Kang, F. Flexible Supercapacitors. *Particuology* **2013**, *11*, 371–377.
- Pushparaj, V. L.; Shajumon, M. M.; Kumar, A.; Murugesan, S.; Ci, L.; Vajtai, R.; Linhardt, R. J.; Nalamasu, O.; Ajayan, P. M. Flexible Energy Storage Devices Based on Nanocomposite Paper. *Proc. Natl. Acad. Sci. U. S. A.* **2007**, *104*, 13574–13577.
- Keskinen, J.; Sivonen, E.; Jussila, S.; Bergelin, M.; Johansson, M.; Vaari, A.; Smolander, M. Printed Supercapacitors on Paperboard Substrate. *Electrochim. Acta* **2012**, *85*, 302–306.
- Lehtimäki, S.; Tuukkanen, S.; Pörhönen, J.; Moilanen, P.; Virtanen, J.; Honkanen, M.; Lupo, D. Low-cost, Solution Processable Carbon Nanotube Supercapacitors and Their Characterization. *Appl. Phys. A: Mater. Sci. Process.* **2014**, *117*, 1329–1334.
- Somov, A.; Ho, C. C.; Passerone, R.; Evans, J. W.; Wright, P. K. Towards Extending Sensor Node Lifetime with Printed Supercapacitors. *Wireless Sensor Networks; Proceedings of the 9th European Conference (EWSN 2012)*, Trento, Italy, Feb 15–17, 2012; pp 212–227.
- Lehtimäki, S.; Li, M.; Salomaa, J.; Pörhönen, J.; Kalanti, A.; Tuukkanen, S.; Heljo, P.; Halonen, K.; Lupo, D. Performance of Printable Supercapacitors in an RF Harvesting Circuit. *Int. J. Electr. Power Energy Syst.* **2014**, *58*, 42–46.
- Jayakumar, H.; Lee, K.; Lee, W. S.; Raha, A.; Kim, Y.; Raghunathan, V. Powering the Internet of Things. *Proceedings of the 2014 International Symposium on Low Power Electronics and Design (ISLPED '14)*, La Jolla, CA, Aug 11–13, 2014; pp 375–380.
- Simon, P.; Gogotsi, Y. Materials for Electrochemical Capacitors. *Nat. Mater.* **2008**, *7*, 845–854.
- Snook, G. A.; Kao, P.; Best, A. S. Conducting-Polymer-Based Supercapacitor Devices and Electrodes. *J. Power Sources* **2011**, *196*, 1–12.
- Chen, J.; Jia, C.; Wan, Z. Novel Hybrid Nanocomposite Based on Poly(3,4-ethylenedioxythiophene)/Multiwalled Carbon Nanotubes/Graphene as Electrode Material for Supercapacitor. *Synth. Met.* **2014**, *189*, 69–76.
- Jacob, D.; Mini, P.; Balakrishnan, A.; Nair, S.; Subramanian, K. Electrochemical Behaviour of Graphene–Poly(3,4-ethylenedioxythiophene) (PEDOT) Composite Electrodes for Supercapacitor Applications. *Bull. Mater. Sci.* **2014**, *37*, 61–69.
- Kumar, A.; Singh, R. K.; Singh, H. K.; Srivastava, P.; Singh, R. Enhanced Capacitance and Stability of *p*-Toluenesulfonate Doped Polypyrrole/Carbon Composite for Electrode Application in Electrochemical Capacitors. *J. Power Sources* **2014**, *246*, 800–807.
- Li, X.; Zhitomirsky, I. Capacitive Behaviour of Polypyrrole Films Prepared on Stainless Steel Substrates by Electropolymerization. *Mater. Lett.* **2012**, *76*, 15–17.
- Li, Y.; Zhao, X.; Xu, Q.; Zhang, Q.; Chen, D. Facile Preparation and Enhanced Capacitance of the Polyaniline/Sodium Alginate Nanofiber Network for Supercapacitors. *Langmuir* **2011**, *27*, 6458–6463.
- Laforgue, A.; Simon, P.; Sarrazin, C.; Fauvarque, J.-F. Polythiophene-Based Supercapacitors. *J. Power Sources* **1999**, *80*, 142–148.

- (19) Elsenbaumer, R.; Jen, K. Y.; Oboodi, R. Processible and Environmentally Stable Conducting Polymers. *Synth. Met.* **1986**, *15*, 169–174.
- (20) Li, L.; Loveday, D. C.; Mudigonda, D. S.; Ferraris, J. P. Effect of Electrolytes on Performance of Electrochemical Capacitors Based on Poly[3-(3,4-difluorophenyl)thiophene]. *J. Electrochem. Soc.* **2002**, *149*, A1201–A1207.
- (21) Poverenov, E.; Li, M.; Bitler, A.; Bendikov, M. Major Effect of Electropolymerization Solvent on Morphology and Electrochromic Properties of PEDOT Films. *Chem. Mater.* **2010**, *22*, 4019–4025.
- (22) Welton, T. Room-Temperature Ionic Liquids. Solvents for Synthesis and Catalysis. *Chem. Rev.* **1999**, *99*, 2071–2084.
- (23) Anderson, J. L.; Ding, J.; Welton, T.; Armstrong, D. W. Characterizing Ionic Liquids on the Basis of Multiple Solvation Interactions. *J. Am. Chem. Soc.* **2002**, *124*, 14247–14254.
- (24) Chakrabarty, D.; Seth, D.; Chakraborty, A.; Sarkar, N. Dynamics of Solvation and Rotational Relaxation of Coumarin 153 in Ionic Liquid Confined Nanometer-Sized Microemulsions. *J. Phys. Chem. B* **2005**, *109*, 5753–5758.
- (25) Damlin, P.; Kvarnström, C.; Ivaska, A. Electrochemical Synthesis and In Situ Spectroelectrochemical Characterization of Poly(3,4-ethylenedioxothiophene) (PEDOT) in Room Temperature Ionic Liquids. *J. Electroanal. Chem.* **2004**, *570*, 113–122.
- (26) Lu, W.; Fadeev, A. G.; Qi, B.; Smela, E.; Mattes, B. R.; Ding, J.; Spinks, G. M.; Mazurkiewicz, J.; Zhou, D.; Wallace, G. G.; MacFarlane, D. R.; Forsyth, S. A.; Forsyth, M. Use of Ionic Liquids for  $\pi$ -Conjugated Polymer Electrochemical Devices. *Science* **2002**, *297*, 983–987.
- (27) Österholm, A. M.; Shen, D. E.; Dyer, A. L.; Reynolds, J. R. Optimization of PEDOT Films in Ionic Liquid Supercapacitors: Demonstration As a Power Source for Polymer Electrochromic Devices. *ACS Appl. Mater. Interfaces* **2013**, *5*, 13432–13440.
- (28) Li, Z.; Cai, J.; Cizek, P.; Niu, H.; Du, Y.; Lin, T. A Self-Supported, Flexible, Binder-Free Pseudo-Supercapacitor Electrode Material with High Capacitance and Cycling Stability from Hollow, Capsular Polypyrrole Fibers. *J. Mater. Chem. A* **2015**, *3*, 16162–16167.
- (29) Stenger-Smith, J. D.; Webber, C. K.; Anderson, N.; Chafin, A. P.; Zong, K.; Reynolds, J. R. Poly(3,4-alkylenedioxothiophene)-Based Supercapacitors Using Ionic Liquids as Supporting Electrolytes. *J. Electrochem. Soc.* **2002**, *149*, A973–A977.
- (30) Liu, D. Y.; Reynolds, J. R. Dioxythiophene-Based Polymer Electrodes for Supercapacitor Modules. *ACS Appl. Mater. Interfaces* **2010**, *2*, 3586–3593.
- (31) Wang, Y.-G.; Li, H.-Q.; Xia, Y.-Y. Ordered Whiskerlike Polyaniline Grown on the Surface of Mesoporous Carbon and its Electrochemical Capacitance Performance. *Adv. Mater.* **2006**, *18*, 2619–2623.
- (32) Kovalenko, I.; Bucknall, D. G.; Yushin, G. Detonation Nanodiamond and Onion-Like-Carbon-Embedded Polyaniline for Supercapacitors. *Adv. Funct. Mater.* **2010**, *20*, 3979–3986.
- (33) Liu, R.; Duay, J.; Lee, S. B. Redox Exchange Induced MnO<sub>2</sub> Nanoparticle Enrichment in Poly(3,4-ethylenedioxothiophene) Nanowires for Electrochemical Energy Storage. *ACS Nano* **2010**, *4*, 4299–4307.
- (34) Groenendaal, L.; Jonas, F.; Freitag, D.; Pielartzik, H.; Reynolds, J. R. Poly(3,4-ethylenedioxothiophene) and Its Derivatives: Past, Present and Future. *Adv. Mater.* **2000**, *12*, 481–494.
- (35) Groenendaal, L.; Zotti, G.; Aubert, P.-H.; Waybright, S. M.; Reynolds, J. R. Electrochemistry of Poly(3,4-alkylenedioxothiophene) Derivatives. *Adv. Mater.* **2003**, *15*, 855–879.
- (36) Sun, Y.; Shi, G. Graphene/Polymer Composites for Energy Applications. *J. Polym. Sci., Part B: Polym. Phys.* **2013**, *51*, 231–253.
- (37) Dreyer, D. R.; Park, S.; Bielawski, C. W.; Ruoff, R. S. The Chemistry of Graphene Oxide. *Chem. Soc. Rev.* **2010**, *39*, 228–240.
- (38) Pei, S.; Cheng, H.-M. The Reduction of Graphene Oxide. *Carbon* **2012**, *50*, 3210–3228.
- (39) Meng, Y.; Wang, K.; Zhang, Y.; Wei, Z. Hierarchical Porous Graphene/Polyaniline Composite Film with Superior Rate Performance for Flexible Supercapacitors. *Adv. Mater.* **2013**, *25*, 6985–6990.
- (40) Zhang, J.; Zhao, X. Conducting Polymers Directly Coated on Reduced Graphene Oxide Sheets as High-Performance Supercapacitor Electrodes. *J. Phys. Chem. C* **2012**, *116*, 5420–5426.
- (41) Yu, C.; Ma, P.; Zhou, X.; Wang, A.; Qian, T.; Wu, S.; Chen, Q. All-Solid-State Flexible Supercapacitors Based on Highly Dispersed Polypyrrole Nanowire and Reduced Graphene Oxide Composites. *ACS Appl. Mater. Interfaces* **2014**, *6*, 17937–17943.
- (42) Lee, S.; Cho, M. S.; Lee, H.; Nam, J.-D.; Lee, Y. A Facile Synthetic Route for Well Defined Multilayer Films of Graphene and PEDOT via an Electrochemical Method. *J. Mater. Chem.* **2012**, *22*, 1899–1903.
- (43) Choi, K. S.; Liu, F.; Choi, J. S.; Seo, T. S. Fabrication of Free-Standing Multilayered Graphene and Poly(3,4-ethylenedioxothiophene) Composite Films with Enhanced Conductive and Mechanical Properties. *Langmuir* **2010**, *26*, 12902–12908.
- (44) Xu, Y.; Wang, Y.; Liang, J.; Huang, Y.; Ma, Y.; Wan, X.; Chen, Y. A Hybrid Material of Graphene and Poly(3,4-ethylenedioxothiophene) with High Conductivity, Flexibility, and Transparency. *Nano Res.* **2009**, *2*, 343–348.
- (45) Kauppinen, J.; Kunnas, P.; Damlin, P.; Viinikanoja, A.; Kvarnström, C. Electrochemical Reduction of Graphene Oxide Films in Aqueous and Organic Solutions. *Electrochim. Acta* **2013**, *89*, 84–89.
- (46) Damlin, P.; Suominen, M.; Heinonen, M.; Kvarnström, C. Non-covalent Modification of Graphene Sheets in PEDOT Composite Materials by Ionic Liquids. *Carbon* **2015**, *93*, 533–543.
- (47) International Electrotechnical Commission. *International Standard: Fixed Electric Double Layer Capacitors for Use in Electronic Equipment*; IEC 62391-1; International Electrotechnical Commission: Geneva, Switzerland, 2006.
- (48) Apilo, P.; Hiltunen, J.; Välimäki, M.; Heinilehto, S.; Sliz, R.; Hast, J. Roll-to-Roll Gravure Printing of Organic Photovoltaic Modules—Insulation of Processing Defects by an Interfacial Layer. *Prog. Photovoltaics* **2015**, *23*, 918–928.
- (49) Kopola, P.; Aernouts, T.; Sliz, R.; Guillerez, S.; Ylikunnari, M.; Cheyns, D.; Välimäki, M.; Tuomikoski, M.; Hast, J.; Jabbour, G.; Mylllä, R.; Maaninen, A. Gravure Printed Flexible Organic Photovoltaic Modules. *Sol. Energy Mater. Sol. Cells* **2011**, *95*, 1344–1347.
- (50) Kawahara, J.; Andersson Ersman, P.; Nilsson, D.; Katoh, K.; Nakata, Y.; Sandberg, M.; Nilsson, M.; Gustafsson, G.; Berggren, M. Flexible Active Matrix Addressed Displays Manufactured by Printing and Coating Techniques. *J. Polym. Sci., Part B: Polym. Phys.* **2013**, *51*, 265–271.
- (51) Hummers, W. S., Jr; Offeman, R. E. Preparation of Graphitic Oxide. *J. Am. Chem. Soc.* **1958**, *80*, 1339–1339.
- (52) Stoller, M. D.; Ruoff, R. S. Best Practice Methods for Determining an Electrode Material's Performance for Ultracapacitors. *Energy Environ. Sci.* **2010**, *3*, 1294–1301.
- (53) Stoller, M. D.; Park, S.; Zhu, Y.; An, J.; Ruoff, R. S. Graphene-Based Ultracapacitors. *Nano Lett.* **2008**, *8*, 3498–3502.
- (54) Du, X.; Guo, P.; Song, H.; Chen, X. Graphene Nanosheets as Electrode Material for Electric Double-Layer Capacitors. *Electrochim. Acta* **2010**, *55*, 4812–4819.
- (55) Lindfors, T.; Österholm, A.; Kauppinen, J.; Pesonen, M. Electrochemical Reduction of Graphene Oxide in Electrically Conducting Poly(3,4-ethylenedioxothiophene) Composite Films. *Electrochim. Acta* **2013**, *110*, 428–436.
- (56) Peng, X.-Y.; Liu, X.-X.; Diamond, D.; Lau, K. T. Synthesis of Electrochemically-Reduced Graphene Oxide Film with Controllable Size and Thickness and Its Use in Supercapacitor. *Carbon* **2011**, *49*, 3488–3496.
- (57) Viinikanoja, A.; Wang, Z.; Kauppinen, J.; Kvarnström, C. Electrochemical Reduction of Graphene Oxide and Its In Situ Spectroelectrochemical Characterization. *Phys. Chem. Chem. Phys.* **2012**, *14*, 14003–14009.
- (58) Viinikanoja, A.; Kauppinen, J.; Damlin, P.; Suominen, M.; Kvarnström, C. In Situ FTIR and Raman Spectroelectrochemical Characterization of Graphene Oxide upon Electrochemical Reduction in Organic Solvents. *Phys. Chem. Chem. Phys.* **2015**, *17*, 12115–12123.

- (59) Ferrari, A. C. Raman Spectroscopy of Graphene and Graphite: Disorder, Electron-Phonon Coupling, Doping and Nonadiabatic Effects. *Solid State Commun.* **2007**, *143*, 47–57.
- (60) Malard, L.; Pimenta, M.; Dresselhaus, G.; Dresselhaus, M. Raman Spectroscopy in Graphene. *Phys. Rep.* **2009**, *473*, 51–87.
- (61) Konwer, S.; Dolui, S. K. Synthesis and Characterization of Polypyrrole/Graphite Composites and Study of Their Electrical and Electrochemical Properties. *Mater. Chem. Phys.* **2010**, *124*, 738–743.
- (62) Bose, S.; Kuila, T.; Uddin, M. E.; Kim, N. H.; Lau, A. K.; Lee, J. H. In-Situ Synthesis and Characterization of Electrically Conductive Polypyrrole/Graphene Nanocomposites. *Polymer* **2010**, *51*, 5921–5928.
- (63) Khomenko, V.; Frackowiak, E.; Beguin, F. Determination of the Specific Capacitance of Conducting Polymer/Nanotubes Composite Electrodes Using Different Cell Configurations. *Electrochim. Acta* **2005**, *50*, 2499–2506.
- (64) Lota, K.; Khomenko, V.; Frackowiak, E. Capacitance Properties of Poly(3,4-ethylenedioxythiophene)/Carbon Nanotubes Composites. *J. Phys. Chem. Solids* **2004**, *65*, 295–301.
- (65) Zubierta, L.; Bonert, R. Characterization of Double-Layer Capacitors for Power Electronics Applications. *IEEE Trans. Ind. Appl.* **2000**, *36*, 199–205.
- (66) Merrett, G. V.; Weddell, A. S. Supercapacitor Leakage in Energy-Harvesting Sensor Nodes: Fact or Fiction? Ninth International Conference on Networked Sensing Systems (INSS), Antwerp, Belgium, June 11–14, 2012; pp 1–5.